EDITORIAL

Geologists have long complained of their low status in the wider culture. A few years ago, one major geological society even convened a working party to consider how this status could be improved.

This is not just a problem of morale. Increasingly science is going to be judged not only by its relevance but also by its popular impact.

Perhaps it is time to bring in the image consultants. First we need to define the problem:

The science is past its philosophical prime

One hundred and fifty years ago geologists were the leading scientific intellectuals because they grappled with philosophical problems at the frontiers of knowledge: the origins of the world, the age of the universe, the origins of life and the origins of man. In the course of the 19th Century all these problems started slipping away from geology: to biology, astronomy, cosmology, and today the only philosophical frontier that could be said to reside (in part) with the Earth sciences (although largely co-opted by the biochemists) is the origin of life.

Yet it continues to offer insights into our world

In the 20th Century the high points of the Earth sciences have concerned our world view: how our planet's continents move, global and local catastrophes and how ice-ages occur. Planetary regulation will remain our dominant contribution to Society. Earthquakes, and other natural catastrophes, continue to have their devilish power to introduce chaos, and metaphorical 'epicentres', 'fault-lines' and the Richter scale have entered popular culture.

Although much of its public face is utilitarian

Where geologists work at the 'front-end' of industry, as in mineral-rich countries such as Australia, Canada, Russia, South Africa or Colombia, or in petroleum-based regions such as the Middle East, Indonesia, Western Norway or North-East Scotland, you will find geoscientists in high status positions: the geologist is perceived as a frontier entrepreneur. You will hear non-geologists at parties in Australia discussing ore grades and mineral rights. Geologists know their potential: one research student sold her field area to a mining company for tens of thousands of dollars before accepting a highly paid job.

However in highly developed countries geologists tend to operate more at the back-end of industry, helping dispose of wastes or clean-up land. It is hard to make this the subject of dinner-party conversation.

Trying to promote the utilitarian virtues of geology can backfire. Two years ago the British Geological Survey, produced a patronizing 1950s-style pamphlet, with a cover showing a grinning 'housewife' being informed how all the items around her home would not be there without geologists. The unintended message was that preconceptions about geologists having poor taste, were correct.

Traditionally geologists had an image problem

The ill-dressed, antisocial geologist, who found rocks easier company than people, was not a good role model. (However with the decline of survey work the reputation of the field geologist is making a comeback.) The information scientist, who happens to work on the Earth, provides the modern ideal. Unlike their laboratory-bound science-colleagues they have life-style advantages heading off to Iceland or Ladakh, when they need to collect some new data. To most people this lifestyle seems relatively glamorous.

Earth scientists seem poor at promoting themselves

To communicate, you have to get inside your audience's heads. Most people find rocks dull. To promote geology widely you have to leave out the rocks and convince people that the medium is not the message.

Science only gets into the papers when it competes with the wars, the murders, and the political scandals. Novelty and relevance are the chief requirements for publicity, followed by topics that touch the soul (astronomers have it easy).

Narrowness of perspective is a primary cause for low esteem. Earth scientists often seem poor at solving total problems, simply focusing on those elements that lie within Earth sciences. If seismologists really wanted to reduce earthquake mortality, they would concentrate on ensuring real changes in building standards.

Status is gained by demonstrating intellectual maturity, by a vision that reaches out to the public and that comprehends and involves the wider culture, of other sciences as well as arts and literature.

Seven tips as to how the Earth Sciences can increase its status:

- accurately predict a volcanic eruption or earthquake;
- die heroically trying to predict a volcanic eruption;
- find an enormous gold deposit;
- become multi-disciplinary problem-solvers for society;.
- become environmental champions;
- organize dangerous expeditions;
- find a Tyrannosaur skeleton with a chunk of meteorite embedded.

TERRA REVIEW

The Morphometric Synthesis for landmarks and edge-elements in images

Fred L. Bookstein
University of Michigan, Ann Arbor, MI 48109, USA

ABSTRACT Over the last decade, techniques from mathematical statistics, multivariate biometrics, non-Euclidean geometry, and computer graphics have been combined in a coherent new system of tools for the biometric analysis of *landmarks*, or labelled points, along with the biological images in which they are seen. Multivariate analyses of samples for all the usual scientific purposes – description of mean shapes, of shape variation, and of the covariation of shape with size, group, or other causes or effects – may be carried out very effectively in the tangent space to David Kendall's *shape space* at the Procrustes average shape. For biometric interpretation of such analyses, we need a basis for the tangent space that is Procrustes-orthonormal, and we need graphics for visualizing mean shape differences and other segments and vectors there; both of these needs are managed by the thin-plate spline. The spline also links the biometrics of landmarks to deformation analysis of curves in the images from which the landmarks originally arose. This article reviews the principal tools of this synthesis in a typical study design involving landmarks and edge information from a microfossil.

Terra Nova, 7, 393–407, 1995.

INTRODUCTION

There used to be two distinct styles of biometric analysis of organic form. In the approach called 'multivariate morphometrics' (e.g. Reyment *et al.*, 1984), conventional multivariate techniques are applied to diverse measures of single forms. The geometric origins of the data play no role in the analytic formalisms ultimately obtained; the only algebraic structures involved are those of multivariate statistics, limited mainly to covariance matrices. These analyses are rarely diagrammatic, and they are rather more useful for ordination than for understanding or theorizing.

In the other class of analyses of form, changes of shape are visualized directly as deformations of Cartesian grids that accord with a pre-assigned biological homology. Whereas in the first approach what correspond from specimen to specimen are the values extracted by ruler or protractor, in the second the concern is with the pairing of 'corresponding' locations of bits of tissue. In spite of many attempts to provide a matching statistical method, these grid analyses remained wholly graphical right through the 1970s (Bookstein, 1978).

Recently these two broad families of techniques have been fused in a surprisingly brief and peaceful methodological development, which I have named *the Morphometric Synthesis*. In the 1980s, Thompson's transformation grids, as applied to landmark configurations, were quantified in a statistically tractable manner. The matrix manoeuvres that had been applied to arbitrary lists of 'shape variables', such as distance-ratios and angles, now could be applied to the explicit geometry of shape without any need for the selection of particular shape variables in advance. Using a newly developed biometric technology of deformation, multivariate findings pertaining to landmark shape proved expressible in geometric diagrams back in the original picture plane. The landmark tactics can be extended to information from outlines and even further to analyses of whole grey-scale images. The resulting morphometric syn-

thesis is of full statistical efficiency, permits explicit tests of many biologically interesting features, and supplies statistical construals for the great variety of graphical techniques that had been previously developed by amateurs.

This synthesis has been announced before, in a monograph (Bookstein, 1991), historical essays (Bookstein, 1993), publications in the jargon of mathematical statistics (e.g. Goodall, 1991, Mardia, 1995), general introductory lectures (Bookstein, 1995a,b,d,e), and three volumes of collected applications, mostly to problems in evolutionary biology and systematics (Rohlf and Bookstein, 1990; Marcus *et al.*, 1993; Marcus *et al.*, 1995). The present paper introduces these strategies to a new audience by re-analysing one dataset from an earlier generation of morphometric innovation: the *Globorotalia* outlines originally sent to me in 1984 by G. P. Lohmann (Woods Hole).

These data (Fig. 1) represent twenty mean shapes of *G. truncatulinoides* carefully synthesized from a much wider range of individual shapes found in dissections of twenty cores from the Indian Ocean floor at latitudes from 16° to 51° S. Lohmann (1983) averaged the forms of each core sample from video silhouettes using his method of 'eigenshapes,' which does not concern us here. (But variants of Lohmann's original approach in which Procrustes distance serves in place of tangent angle still supply one means of constructing average shapes for further statistical analysis: see, for instance, Sampson et al., 1995.) The resulting averages have three clear 'corners' analysed as a triangular shape in Bookstein (1986). Outline information was added in Bookstein (1991), where the midpoints of the outline arcs between landmarks were taken as three additional 'landmarks' (see listing, Bookstein, 1991, p. 406). The representation by edgels is a new digitization for the analysis here.

A BIOMETRIC SHAPE SPACE FOR LANDMARKS

Geometric shape, in the biologist's ordinary language, is what is left of the information in a configuration of k landmarks after one carefully compensates for the effects of *similarity transformations* – changes of geometric position, orientation, and scale. For some time we have had a useful preliminary tool that is invariant against similarity transformations: the *Procrustes distance* between the *shapes* of two landmark configurations. This distance, squared, is usually approximated as the sum of squared distances between corresponding landmarks after each configuration is scaled to unit Centroid Size (sum of squares around its own centroid) and then one of the pair is rotated and translated upon the other so that that interspecimen sum of squares is a minimum.

Using only this Procrustes definition of distance, without any further geometry, the *average shape* can be defined quite rigorously as the shape that has the least summed squared Procrustes distances to the shapes of a sample. Many algorithms have been put forward for computing mean shapes in this least-squares sense. For shape variation of the magnitude that we ordinarily encounter in biometric applications, the various estimates are indistinguishable (Kent, 1995). One popular algorithm begins with an arbitrary but reasonable shape (for instance, that of the first specimen of the sample), Procrustes-fits all the specimens to that one, averages the fitted forms back in the original Cartesian setting, and iterates (Rohlf and Slice, 1990). Others, specific to two dimensional (2D) data, proceed via complex regression (Bookstein, 1991) or eigenanalysis of a Hermitian matrix (Kent, 1994). All are equivalent in the limit of small shape variation.

Multivariate statistical analysis of sampling variation around the average shape requires a more extensive

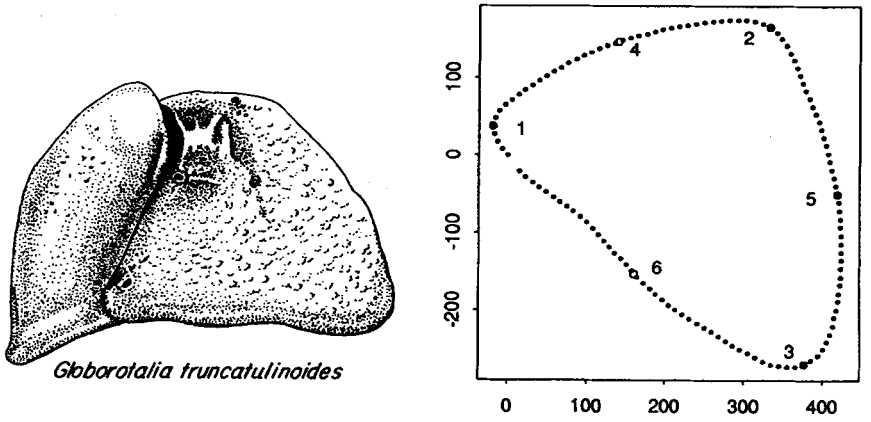

Fig. 1. Globorotalia truncatulinoides. *Left: drawing of a single specimen. Right: typical mean silhouette of the specimens of a single core after the smoothing and singular-value analysis that is Lohmann's (1983) eigenshape analysis (after Bookstein, 1991, fig. 3.4.11). Landmarks 1, 2, 3 are maxima of curvature; points 4, 5, 6 are midway along the arcs between landmarks.*

algebraic structure: *shape coordinates*. Shape coordinates are a set of variables of the correct count ($2k - 4$, for k landmarks in two dimensions; $3k - 7$, in three dimensions) that preserve all the information about shape ordinations and shape statistics in the vicinity of a sample mean. Historically, the first set of shape coordinates to be introduced were Francis Galton's (1907), which I rediscovered in the multivariate context (Bookstein, 1984, 1986). But, except for triangles, these *two-point shape coordinates* did not correspond to any shape metric, and so did not conduce to within-group ordinations, such as principal-components analysis, without strenuous modification. At present, only one simple full-rank system of coordinates preserving the Procrustes metric is known, the *partial warp scores* (Bookstein, 1991) or *weight matrix* (Rohlf, 1993). It is that system that will be introduced and interpreted here. For the (primarily mathematical) argument that all efficient analyses of landmark shape are equivalent to this one in the limit of small shape variation, see Kent, 1995, and Bookstein, 1995a.

Galton's coordinates notwithstanding, the computation of shape coordinates most coherently begins with the Procrustes routines with which we are already familiar (Rohlf and Slice, 1990). If each form of a sample is Procrustes-fitted over the Procrustes average, the 'residuals' that result have, by definition, the correct sum-of-squares (squared Procrustes distance). There are $2k$ of these coordinates, which is four too many, but because they have the correct sum-of-squares, any set of shape coordinates that preserves Procrustes distance (as for the purposes of a principal-components analysis) *must be* a Procrustes-orthogonal rotation of these residuals, and *any* set of shape variables intended to exhaust landmark shape in some ordinary linear multivariate manoeuvre must, like the two-point shape coordinates, derive from these by some possibly anisotropic (skew) linear transformation. This is the unique statistical geometry that underlies the morphometric synthesis: the *a priori* metric geometry of shapes of landmark configurations in Euclidean space[1]. Besides this invariance, these coordinates have several useful elementary properties: for instance, isotropic circular errors of the same variance at each original landmark leave the sample average shape a consistent estimator of the population mean (Kent and Mardia, 1995) and asymptotically result in circular noise at each landmark in these superpositions (Bookstein, 1986; Mardia, 1995).

For our *Globorotalia*, the Procrustes average shape is shown on the left of Fig. 2 and this simplest set of shape coordinates on the right. (Keep in mind that this is not six scatters, one per landmark, but one scatter having eight degrees of freedom masquerading as twelve.) The forms of extreme latitude are indicated. The data clearly suggest that some single factor might be responsible for the variation we see. In other morphometric designs, the object of study might be a group difference, a correlation with some exogenous variable, or some other familiar multivariate contrast or summary vector.

THE THIN-PLATE SPLINE AND THE ORTHONORMAL BASIS FOR SHAPE SPACE

The other major theme of the Synthesis is a praxis for making the geometry of such multivariate patterns explicitly visible in the picture plane (or space) of the typical form. Although D'Arcy Thompson (1917) showed the biologist how transformation diagrams could lead to insight into form, he left no instructions for the production of those drawings from metric or statistical data (Bookstein, 1978). What made the morphometric breakthrough possible was help from an unexpected quarter: a relatively esoteric advance in interpolation theory. The thin-plate spline interpolant we use for *shapes* was originally developed a few years earlier as an interpolant for *surfaces over scattered 'nodes'* at which its height is fixed. In that context, the thin-plate spline is an interpolant that is linear in those 'heights' and that minimizes a global figure of complexity. It is crucial for our purposes, although not for that original application, that that global figure, which is usually called *bending energy*, is a quadratic form in the vector of 'heights'.

The formula for this flexible and intuitively reasonable interpolant has been published many times before, and, as it is not germane to the flow of the exposition here, it is set out in the Appendix.

In the application to 2D landmark data, we compute two of these splined surfaces, one (f_x) in which the vector H of heights is loaded with the x-coordinate of the landmarks in a second form, another (f_y) for the y-coordinate. Then the first of these spline functions supplies the interpolated x-coordinate of the map we seek, and the second the interpolated y-coordinate. The resulting map $(f_x(P), f_y(P))$ is now a deformation of one picture plane onto the other which maps landmarks onto their homologues and has the minimum bending energy of any such interpolant. In this context one may

[1]In its tersest form, this deduction runs as follows. According to Kendall (1984), landmark shapes form a Riemannian manifold with Procrustes distance as metric. Elements of the tangent space to that manifold are functions from linear germs of curves on that manifold into the real numbers: that is what we have always meant by 'shape variables.' Orthonormal shape coordinates are an orthonormal basis for that tangent space at the Procrustes average shape, and hence supply an isometric linearization of sample variation of shape in that vicinity.

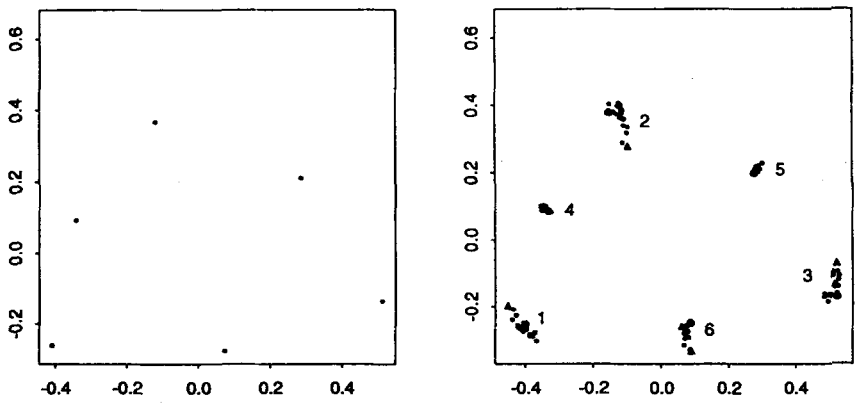

Fig. 2. *Six landmarks from Lohmann's twenty mean* Globorotalia. *(Left) The Procrustes average shape; (Right) the twenty separate core averages in Procrustes registration on the grand mean. Landmarks of the form of lowest latitude are indicated by circles; of highest latitude, by triangles.*

think of 'bending energy' as *localization*, the extent to which the affined derivative of the interpolant varies from location to location. The affine part of the map is now an ordinary shear, which, in the metaphor of the lofted plate, can be thought of as the *shadow* of the original gridded plate after it has been only tilted and rescaled but not bent.

If the landmark coordinates used are actually shape coordinates after the Procrustes fit of the previous section, and if the starting form of the spline is the sample average shape, then we have extended the linear machinery of shape space to a system of diagrams that visualize the relation of any specimen shape to the average as a deformation the coefficients of which are linear in its shape coordinates. In this way Cartesian grids about the average shape have been incorporated into the biometric framework *in toto*, as a direct visualization of one particularly specialized set of linear descriptors.

Figure 3 presents twenty examples of this spline: the deformation representing each of the twenty individual forms (shapes with scale included) as a spline of the grand mean. It is plain to the eye that some sort of trend in shape obtains from low to high latitude (upper left to lower right corner). It certainly looks as if the form goes from bulging upward in the middle, relative to the average, to bulging downward; but our eye is not equipped to discern how complete a description this is. One further crucial tool for the Morphometric Synthesis is an objective procedure by which to arrive at descriptions of such patterns and to assess their explanatory force.

We arrive at that set of descriptors by more closely inspecting the bending-energy quadratic form, the $k \times k$ matrix L_k^{-1} of the Appendix. In general, this matrix has 3 eigenvectors of eigenvalue zero, corresponding to the three-dimensional family of planes over any landmark configuration. There remain $k-3$ dimensions of nontrivial bending above k landmarks, spanned by the nonzero eigenvectors of the bending-energy matrix. These are called *principal warps*. In the spline deformation, each can be imagined lofted as a surface and then projected 'down' onto the picture plane by some two-vector multiple of its 'heights' landmark by landmark and grid intersection by grid intersection. The resulting image, 'shadow' of the principal warp surface in some direction, is called a *partial warp*. The two-vector involved is computed as the inner product of the Procrustes-fit shape coordinates (treated as a complex vector) with the formula of heights of the principal warp, and so is called a *partial warp score*. The principal warps, by their construction as eigenvectors, are orthogonal in the original Euclidean geometry. Because they have no affine part, the corresponding partial warps are orthogonal as shape variables (elements of tangent space to shape space at the average shape) as well (Bookstein, 1995a,e).

These partial warp scores total $2k-6$ shape coordinates. While the spline map remains the sum of all the partial warps together with its own affine term, nevertheless this affine part of the spline is not orthogonal to the partial warps in the Procrustes geometry of shape. A suitably orthogonal term spanning the subspace of uniform shape changes can be denotated as follows (Bookstein, 1995c). Let the Procrustes average shape, scaled to Centroid Size 1 and oriented with principal axes horizontal and vertical, have coordinates $(x_1, y_1), (x_2, y_2), \ldots, (x_k, y_k)$, and let $\alpha = \Sigma x_i^2$ and $\gamma = \Sigma y_i^2$ be the principal moments along those axes. One orthonormal basis for the uniform subspace, which thereby completes a full set of $2k-4$ for the full tangent space, is the pair of Procrustes unit vectors U_n, a $2k \times 2$ matrix, with

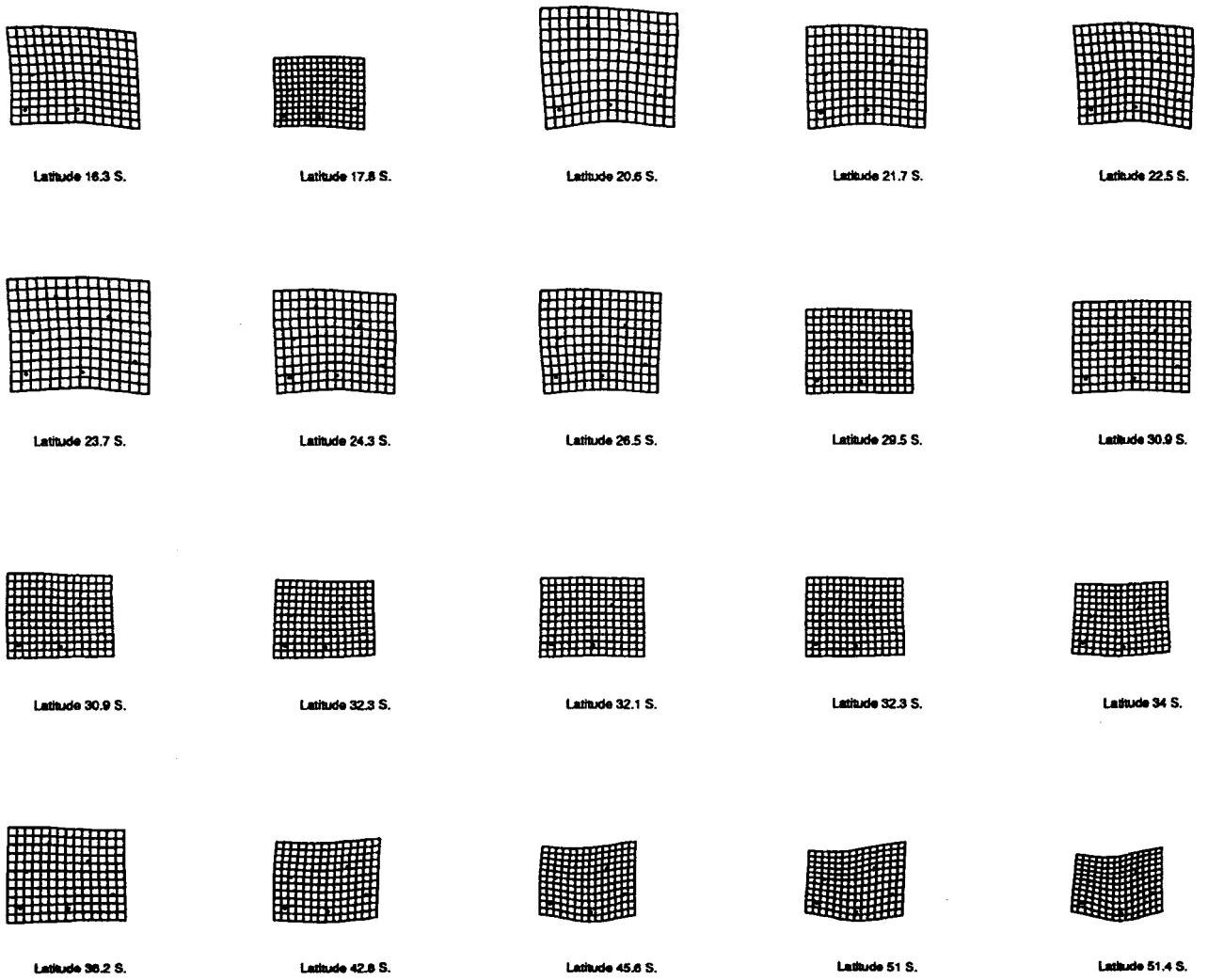

Fig. 3. *Thin-plate splines for deforming the grand mean* Globorotalia *shape into each of the twenty core-specific mean shapes. The mean most closely resembles the form for latitude 29.5° S., second row, fourth column.*

$$Un_1^T = ((\alpha y_1, \gamma x_1), (\alpha y_2, \gamma x_2), \ldots, (\alpha y_k, \gamma x_k))/\sqrt{\alpha\gamma},$$

$$Un_2^T = ((-\gamma x_1, \alpha y_1), (-\gamma x_2, \alpha y_2), \ldots, (-\gamma x_k, \alpha y_k))/\sqrt{\alpha\gamma}.$$

The first of these vectors corresponds to Cartesian shears aligned with the x-axis, the second to Cartesian dilations along the y-axis. It can be shown that the partial warps together with this uniform component constitute an orthogonal rotation of the original set of Procrustes residuals, Fig. 2, into an orthonormal basis for shape space in the vicinity of an average shape. In fact, at present this basis is the only orthonormal basis that has yet been written down (see also Mardia, 1995).

For the *Globorotalia* dataset, this decomposition goes as in Fig. 4. The partial warps are drawn in the lower three panels for horizontal (left) and vertical (right) sets of Procrustes displacements. The top row shows the 'uniform coordinates' that handle the affine term in this same Procrustes metric. Figure 5 shows how a typical deformation grid is the superposition of components of shearing or bending from each of these modes of deformation.

In this way a complete Procrustes-orthonormal basis for shape space is produced from the machinery of the spline. Figure 6 scatters these pairs of partial warp scores for the whole sample of twenty averaged *Globorotalia*. This set of four scatters, which are all to a common scale of Procrustes distance, is an orthogonal rotation of the set of six previously shown in Fig. 2. The four 'missing' dimensions are those that correspond to linearizations of the Procrustes-fit equations—they represent only the curving of the geometry we are linearizing, and have no usable variance for any biometric purpose (see Bookstein, 1995b).

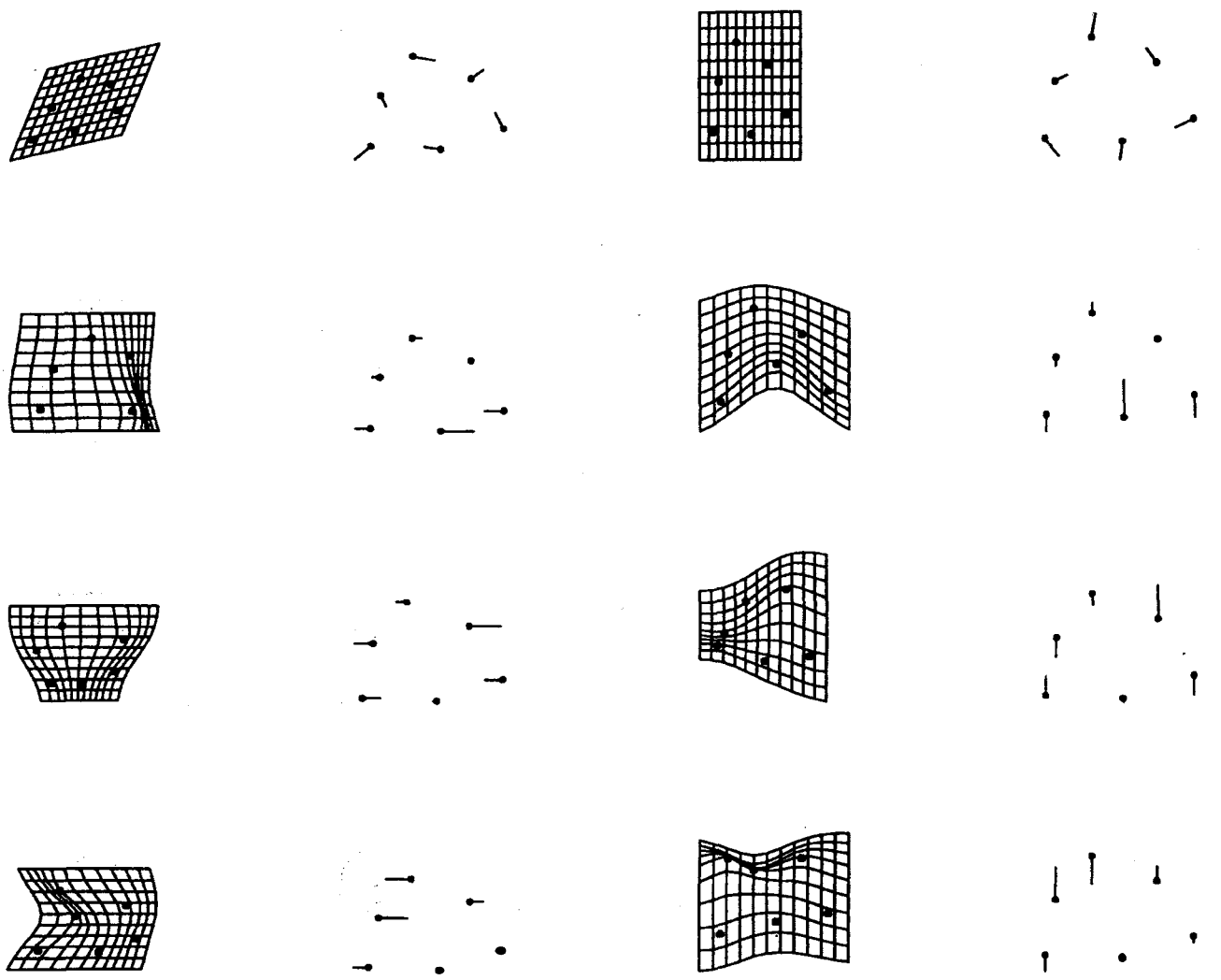

Fig. 4. *The orthonormal shape basis at the average* Globorotalia *shape from Fig. 2. Top row: horizontal and vertical elements of the uniform term, after Bookstein, 1995c. Lower three rows: horizontal and vertical partial warps, least bent (most global) to most bent (most localized). The corresponding shape coordinates are shown to the right of each partial warp. All transformations have Procrustes length 0.3.*

It is now obvious that there is a single factor underlying this sample of shapes. We can compute it as the first *relative* warp (principal component)

$$((-0.23, 0.32), (0.14, -0.39), (0.07, 0.37),$$
$$(-0.03, 0.11), (-0.06, 0.07), (0.11, -0.48))$$

of the Procrustes-fit shape coordinates, Fig. 2, or, exactly equivalently, as the first principal component

$$((0.24, -0.53), (0.17, -0.75), (-0.19, 0.11), (-0.04, 0.13))$$

of their rotation into partial warp scores (Fig. 6). This first component is rigorously interpreted as the shape variable of greatest Procrustes variance per unit Procrustes length of formula. It and the other principal components are computed from covariances, not correlations, because they are already commensurate in units of Procrustes distance, so that no further normalization is of any use (and would, in fact, destroy the interpretation of components like these as extrema of Procrustes variance).

The dominant feature of shape is seen in the second of these vectors of loadings in the second ordered pair of loadings, (0.17, −0.75). This represents the contribution of the partial warp of largest scale, corresponding to the second row in Fig. 4 or the second column in Fig. 6. Graphically, it is manifest in the upward-to-downward-bulge trend in the original spline maps of Fig. 3; we might also have seen it in the parallel vertical displacements of landmarks 2 and 6 in Fig. 2 opposite to the

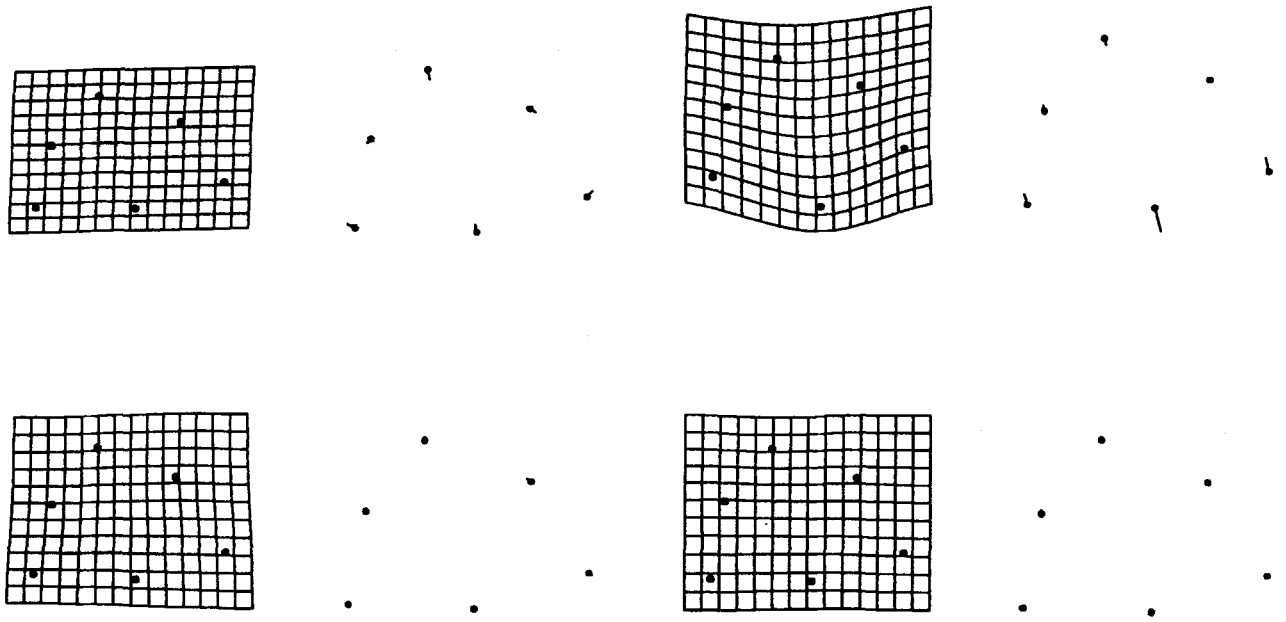

Fig. 5. *How the partial warps combine to generate a thin-plate spline. The full transformation of the sample average shape into the form at latitude 51° S. (Fig. 3, lower right) is the sum of the shear and the three localized bending patterns shown. Each of these three is the sum of multiples of the transformations in the corresponding rows of Fig. 4. Partial warp scores, beginning with the uniform component:* $((0.028, -0.073), (0.030, -0.114), (-0.025, 0.018), (-0.002, 0.020))$.

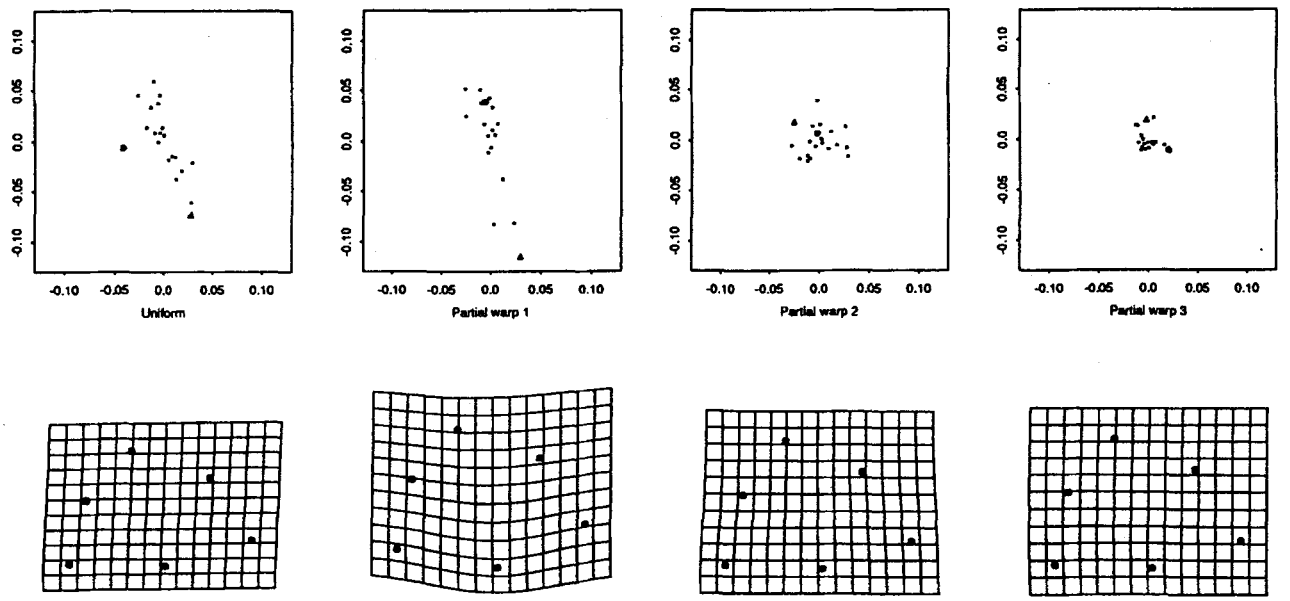

Fig. 6. *Partial warp scores for the* Globorotalia *dataset. (above) Scatters for the uniform component and the three partial warp scores. All axes are commensurate in units of Procrustes length. The forms of highest and lowest latitude are indicated by the same symbols as in Fig. 2. Notice that the form of lowest latitude is an outlier on the uniform component, as is also visible, in hindsight, in Fig. 3. (below) Partial warps for the transformation from the mean of the first ten forms (see Fig. 2) to that of the last ten forms.*

vertical displacements of the left and right corners 1 and 3. From the expression to the basis of Procrustes residuals we see how little the residuals at landmarks 4 and 5 contribute to this component – no loading is

greater than 0.11 – as was already hinted in Fig. 2. Beyond that largest principal warp, the other set of loadings incorporates considerable correlated variation in the uniform component (Fig. 6, leftmost column), the value −0.53 connoting a vertical compression with latitude. Contributions from features at the two smaller scales are negligible.

The columns of Fig. 6 represent the partial warps as a basis for shape space. At the same time, they combine graphically, just as in Fig. 5, to represent any shape signal as a deformation. The technique demonstrated there for the single specimen at the lower right-hand side in Fig. 3 serves to construct a deformation visualizing *any* multivariate feature vector arising out of that same basis treated as pertaining to shape coordinates in the vicinity of the average shape. For instance, while contemplating our first principal component, we are not restricted to its expression as a vector of loadings in one basis or another, as set out two paragraphs above. The same vector in shape space may be visualized directly as a deformation: a linear combination of multiples of the partial warps (Fig. 4), superposed by addition. (That is why those principal components were called 'relative warps' above.)

Figure 7 shows this first component both as a deformation and as a Procrustes-fit pattern. The second component, also shown, explains only 9% as much Procrustes variance. The sample scatter, at the right, confirms that this data set is, in effect, one-dimensional. By retracing the chain of reinterpretations these data have undergone, we can identify that scatter as pertaining to a *principal coordinates analysis of intra-sample Procrustes distance* (Reyment & Jöreskog, 1993). (Such simplicity does not always obtain, however; for more complicated examples, see Bookstein, 1995a,d.) For these *Globorotalia*, this first component appears to combine two geometrically distinct trends: an increase in the conical angle with latitude, as originally reported in Lohmann (1983), and a rise in the keel with latitude, as reported in Bookstein (1991). These are carried by the uniform component and the first partial warp, the first and second columns in Fig. 6.

Principal component analysis is only one of many multivariate analyses that can all go forward in this same set of coordinates. Not all of them require this specific basis, but, rather, different multivariate techniques place different requirements on one's selection. For instance, a Hotelling's T^2 or MANOVA requires a selection of $2k - 4$ shape coordinates, but any full-rank set, such as my earlier two-point coordinates, will do: the Procrustes metric is no longer relevant. Correlation with Centroid Size or with an outside 'cause' or 'effect' of shape can be graphed according to any rotation of the Procrustes fit coordinates. The two-point basis is easiest to draw, but doesn't suggest a shape metric or conduce easily to principal component analysis, and so on.

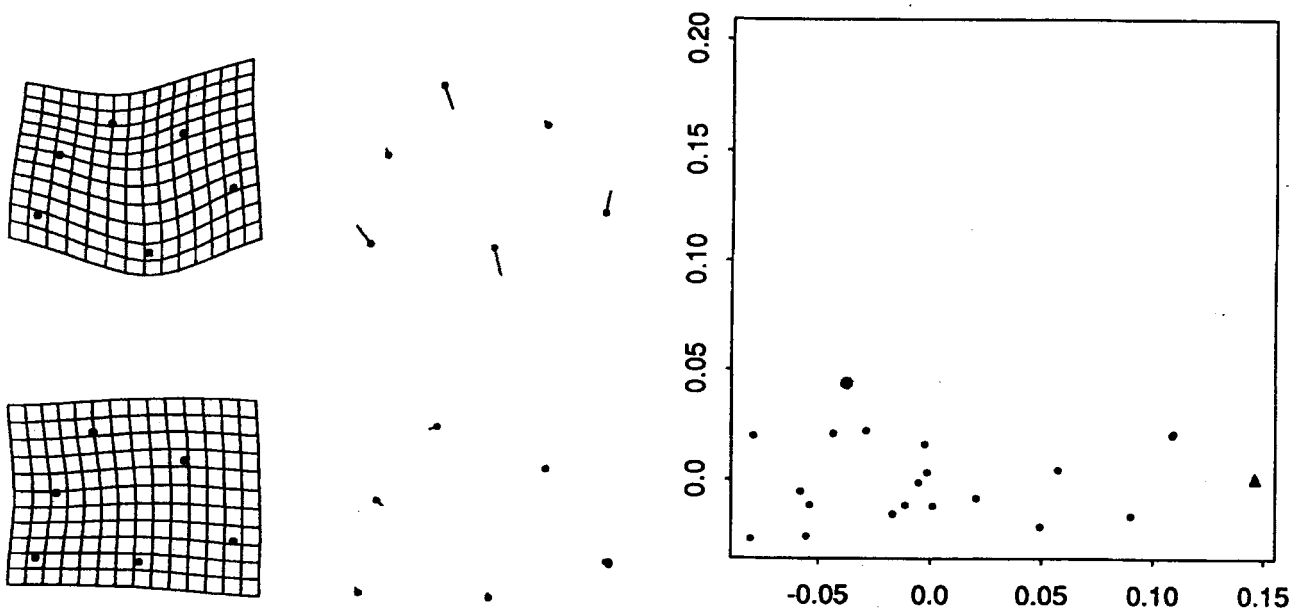

Fig. 7. *Principal components of the* Globorotalia. *Left, relative warps 1 and 2, as thin-plate splines of the mean corresponding to the full sample range of scores. Top, component 1 (compare the extreme forms at upper left and lower right in Fig. 3); bottom, component 2. Centre, the same components drawn as vectors of displacement in shape space. (Recall this sort of diagram pertains to one vector, not six.) Right, sample scatter on these two components; the second explains only 9% as much variation as the first. This plot is equivalent to the scatter of the first two principal coordinates of Procrustes distance for these forms.*

Only a skew basis is required, for instance, to test for association of the *Globorotalia* shapes with latitude. Compute shape coordinates as shown in Fig. 8, the locations of landmarks 2 and 4 through 6 when #1 and #3 are fixed in position. Summed squared scatters in this registration are almost always obviously worse than that in the Procrustes registration (Fig. 2). The test for independence of this vector of eight shape variables from latitude is the *F*-test corresponding to the multiple regression of latitude upon these eight. (But the coefficients in the multiple regression have no meaning.) That multiple correlation is 0.9303; its significance is not in doubt. The association is visualized as the relation between the sample average shape and one that differs from it by adjustments of each shape coordinate according to its own separate prediction by latitude. The consequences for shape of two standard deviations of change in latitude seen in Fig. 8 (right), confirm the unidimensional structure of these microfossils by its resemblance to the shape in Fig. 7 (upper left). Note, also, the visual effect of rotating the grid; the partial warp scores themselves are standardized against such rotations.

The invariance of these techniques of exogenous covariance against oblique change of basis is easy to demonstrate algebraically or geometrically. In Fig. 9 we compute the same correlation with latitude to a badly flawed shape coordinate basis, the two-point registration on landmark 1 and neighboring pseudolandmark 6. The multiple correlation remains 0.93, and the 'predicted shape' differs from that in the preceding figure only in size and orientation. As another special case, if the affine term is known in advance to be nuisance variation (for instance, in most studies of human brain anatomy), one might restrict one's analysis solely to the *nonuniform subspace*, that resulting from

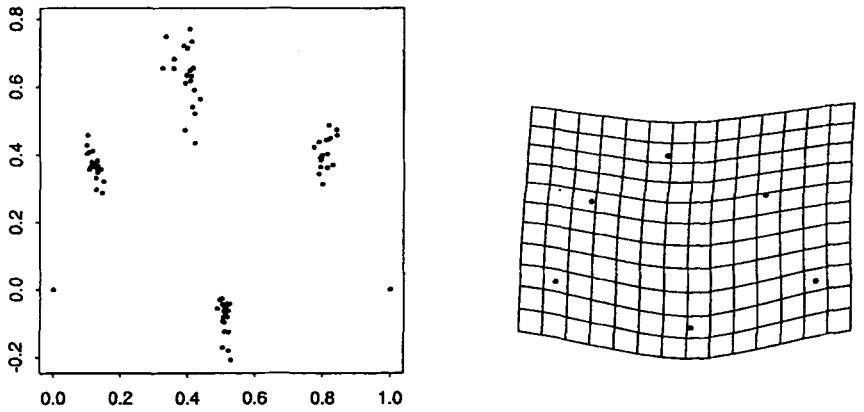

Fig. 8. *Left: one set of shape coordinates for the* Globorotalia *dataset, to a baseline from landmark landmark 1 to landmark 3. While the shapes are much more widely scattered on the page than those of Figure 2, their multivariate statistics are virtually unchanged. Right: shape change induced by two standard deviations of change in latitude on these shape coordinates.*

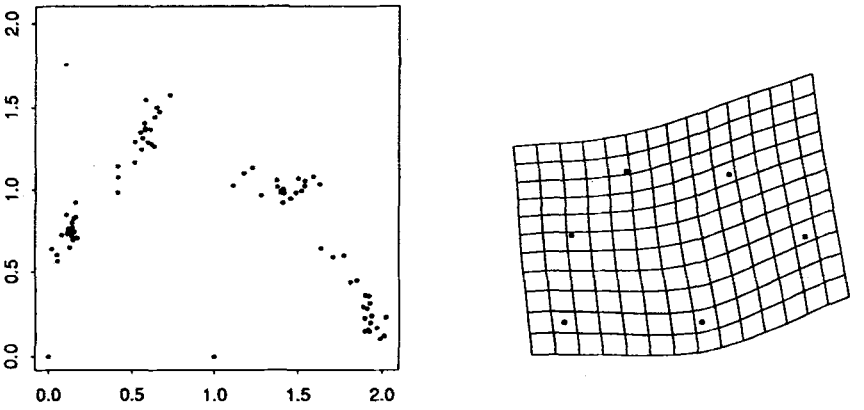

Fig. 9. *The same shape regression according to another shape basis, with baseline from landmark 1 to landmark 6. Left, the new basis, an inappropriate set of shape coordinates (note enormous, curving scatters); right, the regression on latitude, indistinguishable from that in the preceding figure.*

deleting the subspace of shears and dilations diagrammed at the far left in Fig. 6. Within this subspace, some analyses treat different scales of shape differently: for instance, 'relative warps analysis with $\alpha = -1$' (Rohlf, 1993), which is a principal-coordinates analysis of bending energy itself. These and other choices are all reviewed in Bookstein, 1995b. Still other modified bases apply to nearly symmetric forms (op. cit.).

It is not necessary that a diagram display all dimensions of this space for it to be useful. Figure 10, for instance, shows the 'residuals' characterizing *Globorotalia* shape when all three of the original corner landmarks (Fig. 1) are fixed at their average positions. This plot is no longer in Procrustes registration, but there is a compensation: that striking concentration of the nonlinearity at landmark 6, a concentration more typical of resistant-fit superpositions (Rohlf and Slice, 1990) than the linear manoeuvres here.

EDGELS

Beyond landmarks, there is another traditional source of quantitative data about organic form: the shapes by which biological objects bound themselves as systems in space. These shapes are the curves in two dimensions, surfaces in three, that we call biological *outlines*. In parallel with the early developments of methods for analysis of landmarks, multivariate methods were developed for analysis of outline information, most often for 2D data but sometimes, as in phrenology, in

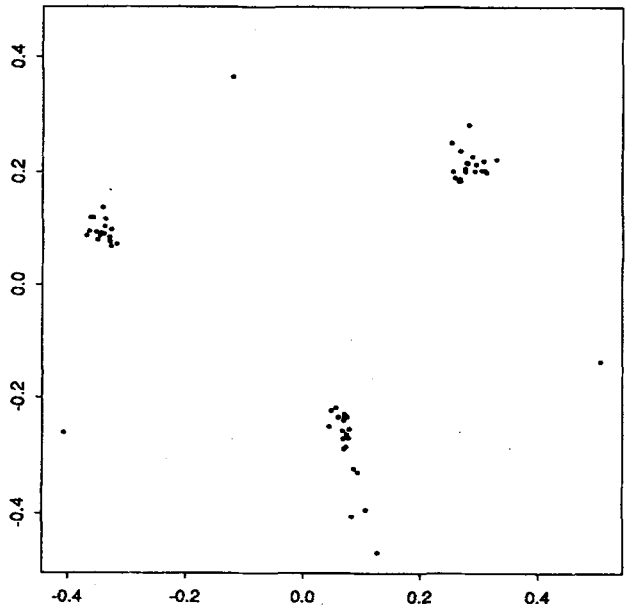

Fig. 10. *Scatter of the* Globorotalia *after an affine registration upon the three corner landmarks. Notice the concentration of variation at landmark 6.*

three dimensions. On the whole, these attempts have failed. Different systems of parameterization give rise to incommensurate inter-specimen distances that seem to have very little biological signal in common (Rohlf, 1990). For instance, Lohmann's (1983) eigenshape method, which produced the outlines from which the landmarks of this example were actually taken, nevertheless itself has no way of referring to those landmarks. Some very recent methods of image analysis (Grenander *et al.*, 1991; Grenander and Miller, 1994) can use both landmarks and outlines for image analyses one at a time; perhaps these approaches will soon have a biometrical component as well.

Until then, we are stuck with a complete incommensurability between two traditions of analysis of the same images. This divergence is very inconvenient. Many landmarks (for instance, numbers 4, 5, and 6 here) actually serve to encode information about curves instead. These are the landmarks called 'Type III' in Bookstein (1991): points such as extremes of diameters or touching points of double tangents, having operational definitions that refer to more than one region of an outline. And other landmarks that are perfectly well characterizable by local features of form nevertheless lie on curves. Reducing the available information about such a scene to a mere pair of Cartesian coordinates loses information about the orientation of that curving element through the landmark. In three dimensions, even more information is lost: not only the orientation of the normal planes to surfaces on which landmarks can lie, but the more informative orientation of tangent lines to curves in three dimensions, such as the 'corners' of the eye. Averaging works for these representations (Cutting *et al.*, 1993; Dean and Marcus, 1995), but so far no more sophisticated feature spaces have been supplied.

Instead we have managed to treat curves as generalized landmarks in a method tied together by some calculus springing from the splines. Very recently methods have been developed for the incorporation of information about curving form in the same two-metric context (Procrustes distance alongside bending energy) that has proved so fertile a methodology for landmark data. We model information about a direction through a landmark by using extra landmarks in a very carefully controlled way: via a formal element, the *edgel* (edge-element), that is a pair of landmarks at fixed orientation and unknown but very small separation. Figure 11, for instance, augments the familiar *Globorotalia* form by edgels at three of the landmarks. The orientation of those edgels is presumed to have been measured on each specimen at some fixed geometric scale. As a set of parameters, then, each adjacent pair of 'landmarks' is carrying one invariable coordinate that should not be

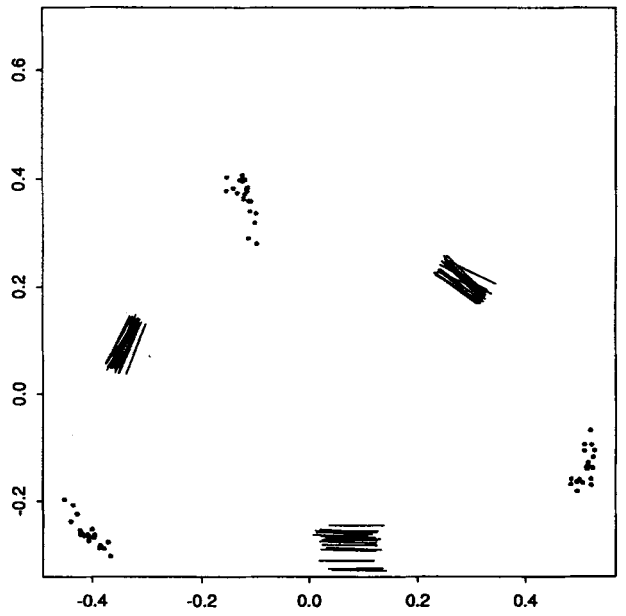

Fig. 11. *Extension of the* Globorotalia *data set by three edgels at original landmarks 4, 5, 6, shown in the same Procrustes registration as was used in Fig. 2. The length of the edgels as drawn is arbitrary.*

allowed into the data analysis. It turns out that the entire matrix algebra of the synthesis, splines and all, can be extended to arbitrary mixtures of landmarks of this artificially enriched type along with ordinary ones. (Using an identical algebraic strategy but a rather more complicated notation, the extension goes further, allowing any specification of the affine derivative of the spline map at a landmark. See Bookstein and Green, 1993b.)

One way to preclude that superfluous coordinate from disturbing our biometrics is to hold it constant by explicit algebraic control. The constancy does not apply in the original digitizing plane, but, as in Fig. 11, after projection down into the space of shape coordinates near the average shape[2]. Once the landmarks have been fitted to the mean shape, we can remove the 'redundant' coordinate permanently. The biometrics of the resulting extended 'landmarks' now extends the biometrics of the original ones by one coordinate per edgel. In this way we can extend all linear modelling involving landmarks – all group differences or covariances with causes or effects of form – to include whatever additional information about outlines is available, either as predictor or as graphical element.

But we can do a great deal better than this somewhat inelegant incorporation of edge-directions as addenda to shape space: they can enter into the formalism of Procrustes distance and bending energy quite explicitly. Bookstein and Green (1993*a*) show in detail how the space of principal warps introduced above – the orthonormal basis for our biometrics – behaves when landmarks are introduced in restricted pairs in this manner and thereafter the separation between the elements of the pairs is sent to zero even while the 'aperture' at which those orientations are observed remains constant. The maps that emerge, *singular perturbations* of the original thin-plate spline for landmarks, seem novel to this application. In the limit, the original space of partial warps of landmarks is reconstituted, accompanied by a new, Procrustes-orthogonal space of shape variation pertaining only to edgels. The shapes in this subspace are the spline pullbacks of the original edgels onto the Procrustes average shape for the actual landmarks. There are two metrics in this subspace, a Procrustes metric and a bending metric; each is inherited unmodified from the general formalism except for indeterminate multipliers of proportionality. The Procrustes metric is here equivalent to a sum of squared rotations; the bending metric becomes the additional bending energy contributed to the total for the spline by the reorientation of edgels.

As for the original thin-plate spline, the formulae for these maps do not contribute to my main argument; they have been relegated to the Appendix.

The *Globorotalia* data set can be extended by outline directions at three of its six landmarks. Figure 11 has already shown this newly augmented data set, with each edgel represented by a segment of visually convenient length, in Procrustes registration on the landmarks. The variances of the edgels here are 0.0038, 0.0132, 0.00026 squared radians; the dominance of the second is plain in the picture. Figure 12 shows the Procrustes average landmark locations and the variation in edgel direction that remains after each specimen is splined onto the landmark average shape using all six landmarks, even the ones under the edgels. Here the variances of the edgels are 0.0016, 0.0026, 0.0010 squared radians, and total residual variation is 0.0052 squared radians per form, versus 0.0173 in the Procrustes registration. Most of this edgel variance is already stabilized in the affine registration at the corner landmarks alone (Fig. 13—the same superposition as in Fig. 10).

In a principal-components analysis of the edgels in this landmarks-only registration, a first component, (0.50,0.79,-0.35), accounts for 71% of the Procrustes variance of edgels. This is the conjoint rotation of edgels 1 and 2 together with some additional opening of the curvature at landmark 3. The score on this component

[2]In computing the average, the duplicated landmarks do not carry doubled weight.

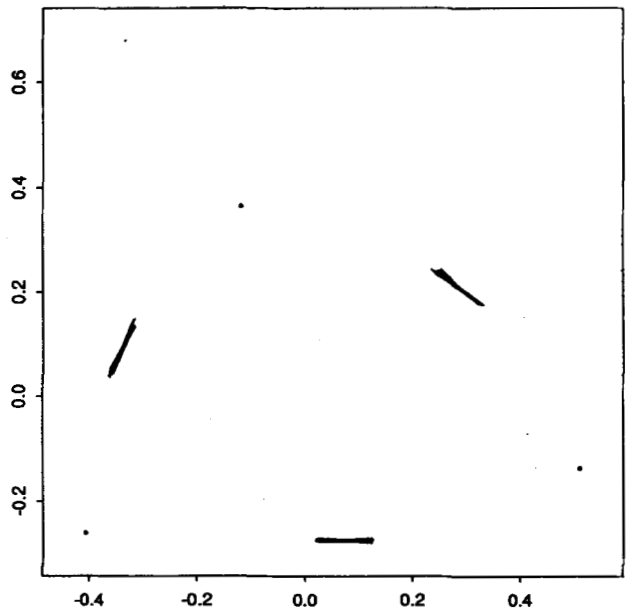

Fig. 12. *Residual edgel variance after all six landmarks are pulled back to their mean positions by splines.*

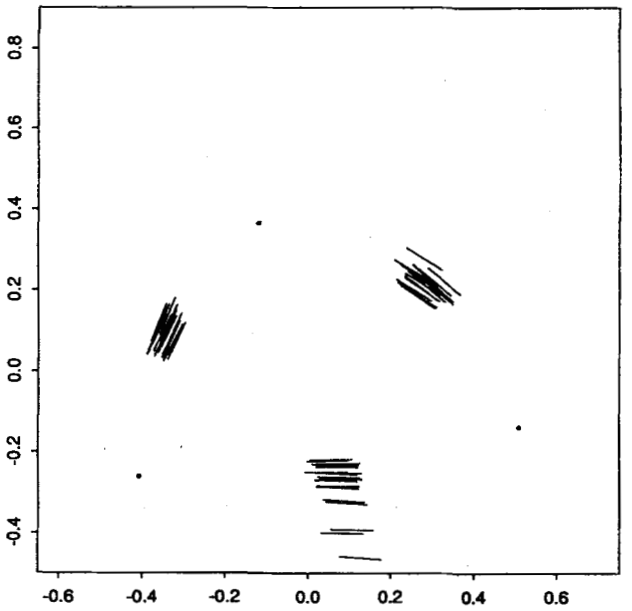

Fig. 13. *Edgel locations after only the corner landmarks are pulled back.*

correlates 0.763 with the uniform component of landmark shape (the principal component of the landmarks on which Fig. 10 was actually registered), 0.825 with the first principal component of shape for all six landmarks, and 0.747 with latitude, our proxy for that general factor: higher latitudes, more clockwise rotations at edgels 1 and 2.

For this set of landmarks and mean orientations, the bending energy matrix $\tilde{N}$ for edgels (see the Appendix) is

$$\begin{pmatrix} 1.428 & 0.011 & -0.011 \\ 0.011 & 1.030 & -0.010 \\ -0.011 & -0.010 & 0.828 \end{pmatrix}.$$

Its structure is nearly diagonal because the form is nearly an equilateral triangle with edgels at midpoints of sides, for which the edgel-bending energy matrix must be, by symmetry, a multiple of the identity. The magnitudes down the diagonal of this matrix are inverse to the lengths of the sides of the triangle: the shorter the side, the more energy it takes to twist it into an *S*-curve.

A spline leaving the landmarks fixed and expressing a suitable multiple of their coordinated rotations with latitude is shown in Fig. 14. In spite of the small magnitude of the edgel changes, they incorporate as much predictive information about shape change as do the landmarks on which they lie. Figure 15 indicates the 'prediction' of landmark locations from solely the first principal component of the edgel-directions from Fig. 12 (cf. Fig. 7, upper left), a prediction from the first principal component of landmark shape itself; but no information about covariances among shape coordinates of landmarks was available to the edgel predictor. The information content of the edgels and the landmarks underlying them is almost equivalent. A startling realization, but not paradoxical: those last three 'landmarks' never really were homologous locations, but only markers evenly dividing arc-length between the corners.

In the same way that landmarks serve both as a tool for standardizing images and as a biometric database in

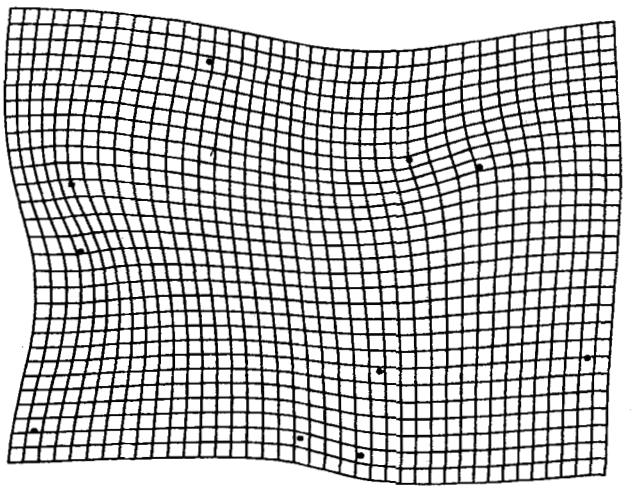

Fig. 14. *Effect of latitude upon edgel orientations in Fig. 13, scaled to a sufficiently large number (20) of standard deviations of latitude to be legible on the page.*

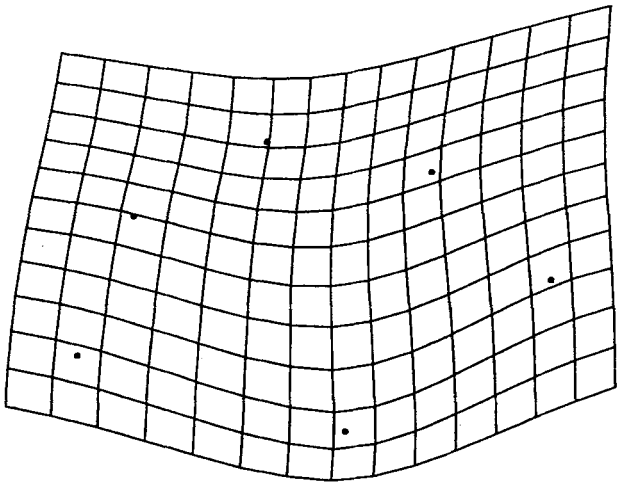

Fig. 15. *Prediction of landmark shifts given by the first principal component of edgel-rotation (cf. Fig. 7).*

their own right, edgels have a second role as a tool for further standardizing those images when curving structures are plausibly taken as homologous between images. Combinations of landmarks and edgels supply a remarkably flexible context for digitizing scenes of some complexity (see Bookstein and Green, 1994a, or Bookstein, 1994, for more tools and examples). William Green's program package edgewarp for Unix workstations (Bookstein and Green, 1994b) includes a complete facility for the edgel manoeuvres here, for applying all these computations to images containing landmarks, and for many other geometric variants. It may be obtained by FTP from brainmap.med.umich.edu. Follow the instructions in the README file in the /pub/edgewarp directory.

ACKNOWLEDGEMENTS

The exposition here has been worked out over several years of teaching at workshops jointly taught by Les Marcus, Jim Rohlf, and Richard Reyment. Much of the research reported here was underwritten in part by NIH grants DA–09009 and GM–37251 to Fred L. Bookstein. The first of these grants is jointly supported by the National Institute on Drug Abuse, the National Institute of Mental Health, and the National Institute on Aging as part of the Human Brain Project. I thank G. P. Lohmann, WHOI, for the original *Globorotalia* outlines.

APPENDIX: FORMULATIONS OF THE THIN-PLATE SPLINE

This Appendix collects the formulae by which thin-plate splines are produced from landmark data and from edgel data.

The thin-plate spline interpolant for landmarks (Bookstein, 1989)

Let U be the function $U(\vec{r}) = r^2 \log r$, and consider a reference shape (in practice, a sample Procrustes average) with landmarks $P_i = (x_i, y_i), i = 1, \ldots, k$. Writing $U_{ij} = U(P_i - P_j)$, build up matrices

$$K = \begin{pmatrix} 0 & U_{12} & \ldots & U_{1k} \\ U_{21} & 0 & \ldots & U_{2k} \\ \vdots & \vdots & \ddots & \vdots \\ U_{k1} & U_{k2} & \ldots & 0 \end{pmatrix}, \qquad Q = \begin{pmatrix} 1 & x_1 & y_1 \\ 1 & x_2 & y_2 \\ \vdots & \vdots & \vdots \\ 1 & x_k & y_k \end{pmatrix},$$

and

$$L = \begin{pmatrix} K & Q \\ Q^T & O \end{pmatrix}, (k+3) \times (k+3),$$

where O is a 3×3 matrix of zeros. The thin-plate spline $f(P)$ having heights (values) h_i at points $P_i = (x_i, y_i)$, $i = 1, \ldots, k$, is the function

$$f(P) = \sum_{i=1}^{k} w_i U(P - P_i) + a_0 + a_x x + a_y y,$$

where

$$W = \begin{pmatrix} w_1 & \ldots & w_k & a_0 & a_x & a_y \end{pmatrix}^T = L^{-1} H$$

with

$$H = \begin{pmatrix} h_1 & h_2 & \ldots & h_k & 0 & 0 & 0 \end{pmatrix}^T.$$

Notice that this vector W is linear in the data H of 'heights'.

Then the function $f(P)$ has three crucial properties.
(i) $f(P_i) = h_i$, all i: f interpolates the heights h_i at the landmarks P_i.
(ii) The function f has minimum *bending energy* of all functions that interpolate the heights h_i in that way: the minimum of

$$\iint_{\mathbf{R}^2} \left(\left(\frac{\partial^2 f}{\partial x^2} \right)^2 + 2 \left(\frac{\partial^2 f}{\partial x \partial y} \right)^2 + \left(\frac{\partial^2 f}{\partial y^2} \right)^2 \right),$$

where the integral is taken over the entire picture plane.
(iii) The value of this bending energy is

$$\frac{1}{8\pi} W^T H = \frac{1}{8\pi} H_k^T L_k^{-1} H_k,$$

where L_k^{-1}, the *bending energy matrix*, is the $k \times k$ upper left submatrix of L^{-1}, and H_k is the corresponding k-vector of 'heights' $(h_1 \quad h_2 \quad \ldots \quad h_k)$.

The thin-plate spline for edgels (Bookstein & Green, 1993a)

Recall the kernel function $U(\vec{r}) = r^2 \log r$ of the original

thin-plate formalism (previous section). Let there be k ordinary landmarks $P_1, \ldots, P_k$ and m edgels having mean orientations t_j (unit vectors) at points P_{i_j}, $j = 1, \ldots, m$. By this we mean the limiting form of a spline on landmarks at the points P_{i_j} and also at points $P_{i_j} + \delta t_j$ as $\delta \to 0$. For any unit vector t, let U_t denote the derivative of the kernel U at z in the direction of t. Then

$$U_{t_j}(z) = t_j \cdot \nabla U(z) = (2 \log |z| + 1)(z \cdot t_j).$$

Similarly, the second derivative $(U_t)_u$ will be denoted $U_{t,u}$. Explicitly,

$$U_{t_i,t_j}(z) = t_j \cdot \nabla U_{t_i}(z) = \frac{2}{|z|^2}(z \cdot t_i)(z \cdot t_j) + (2 \log |z| + 1)(t_j \cdot t_i).$$

By convention these both return 0 for argument $z = 0$. In addition to K, we need two other matrices expressing the geometry by which the edgels relate to the landmarks and to each other:

$$K_1 = \begin{pmatrix} U_{t_1}(P_1 - P_{i_1}) & \ldots & U_{t_m}(P_1 - P_{i_m}) \\ U_{t_1}(P_2 - P_{i_1}) & \ldots & U_{t_m}(P_2 - P_{i_m}) \\ \vdots & & \vdots \\ U_{t_1}(P_k - P_{i_1}) & \ldots & U_{t_m}(P_k - P_{i_m}) \end{pmatrix}$$

and

$$K_2 = \begin{pmatrix} U_{t_1,t_1}(P_{i_1} - P_{i_1}) & \ldots & U_{t_m,t_1}(P_{i_1} - P_{i_m}) \\ U_{t_1,t_2}(P_{i_2} - P_{i_1}) & \ldots & U_{t_m,t_2}(P_{i_2} - P_{i_m}) \\ \vdots & & \vdots \\ U_{t_1,t_m}(P_{i_m} - P_{i_1}) & \ldots & U_{t_m,t_m}(P_{i_m} - P_{i_m}) \end{pmatrix}.$$

Also, define

$$V = \begin{pmatrix} 0 & t_{1,x} & t_{1,y} \\ \vdots & \vdots & \vdots \\ 0 & t_{m,x} & t_{m,y} \end{pmatrix},$$

and

$$M = \begin{bmatrix} -K_1 \\ \hline V^T \end{bmatrix}.$$

Then the edge-driven spline differs from the landmark-only spline by the addition of a term that can be approximated as

$$f_1(z) = \sum_{i=1}^{n} w_{1,i} U(z - P_i) - \sum_{j=1}^{m} e_{1,j} U_{t_j}(z - P_{i_j}) + a_{1,1}x + a_{1,2}y + a_{1,3},$$

where

$$e_1 = \frac{-1}{2 \log \delta}\left(\mathrm{I}_m + \frac{N}{2 \log \delta}\right)^{-1} \Delta s$$

and

$$\begin{pmatrix} w_1 \\ a_1 \end{pmatrix} = -L^{-1} M e_1.$$

Here Δs is a vector of slope changes Δs_j at each edgel P_{i_j}, and $N = K_2 + M^T L^{-1} M$ is the *bending-energy matrix for edgels*, the expression that organizes all their energetics.

As the edge length $\delta \to 0$, all these approximations are accurate to $O(-\delta \log \delta)$ or better.

For instance, the contribution that a shear of slope Δs_j at each landmark makes to the bending energy of the resulting lofted surface, is, approximately, $(-2 \log \delta)^{-2} \Delta s^T N \Delta s$, along with a term in $(-2 \log \delta)^{-1} \|\Delta s\|^2$; the additional bending cost of rotation of each edgel by an angle $\Delta \theta_j$ in plane is approximately $(-2 \log \delta)^{-2} \Delta \theta^T \widetilde{N} \Delta \theta$, where $(\widetilde{N})_{ij} = (t_i \cdot t_j) N_{ij}$, along with a term in $(-2 \log \delta)^{-1} \|\Delta \theta\|^2$.

Within the subspace of edgel information, an orthonormal basis of principal warps (eigenvectors of bending with respect to Procrustes distance) can be produced by eigenanalysis of $\widetilde{N}$ just as we did for landmarks by eigenanalysis of L_k^{-1}. These principal edgel warps emerge as coordinated rotations of all the edgels at once having unit Procrustes length and maximum, minimum, or stationary values of bending energy. (There is no analogue to the uniform component of shape change for edgels.)

REFERENCES

Bookstein F.L. (1978) *The Measurement of Biological Shape and Shape Change*. Lecture Notes in Biomathematics, vol. 24. Springer, New York.

Bookstein F. L. (1985) Tensor biometrics for changes in cranial shape, *Annls Hum. Biol.*, **11**, 413–437.

Bookstein F.L. (1986) Size and shape spaces for landmark data in two dimensions, *Stat. Sci.*, **1**, 181–242.

Bookstein F.L. (1989) Principal warps: thin-plate splines and the decomposition of deformations, *IEEE Trans. Pattern Analysis Machine Intelligence*, **11**, 567-585.

Bookstein F.L. (1991) *Morphometric Tools for Landmark Data*. Cambridge University Press, New York.

Bookstein F.L. (1993) A brief history of the morphometric synthesis. In: *Contributions to Morphometrics* (ed. by L. Marcus, E. Bello and A. García-Valdecasas), pp. 15–40. Monografias, Museo Nacional de Ciencias Naturales, Consejo Superior de Investigaciones Cientificas, Madrid.

Bookstein F.L. (1994) Landmarks, edges, morphometrics, and the brain atlas problem. In: *Functional Neuroimaging: Technical Foundations* (ed. by R. Thatcher, M. Hallett, T. Zeffiro, and E.R. John, pp. 107–119. Academic Press, New York.

Bookstein F.L. (1995a) The morphometric synthesis: A statistical praxis for biomedical images with landmarks, *Stat. Sci.*, in review.

Bookstein F.L. (1995b) Combining the tools of geometric morphometrics. In: *Advances in Morphometrics: Proc. 1993 NATO ASI Morphometrics* (ed. by L.A. Marcus *et al.*). Plenum, in press.

Bookstein F.L. (1995c) A standard formula for the uniform shape component in landmark data. In: *Advances in Morphometrics: Proc. 1993 NATO ASI on Morphometrics* (ed. by L. Marcus *et al.*). Plenum, to appear.

Bookstein F.L. (1995d) Biometrics, biomathematics, and the morphometric synthesis, *Bull. Math. Biol.*, accepted pending revisions.

Bookstein F.L. (1995e) Metrics and symmetries of the morphometric synthesis. In *Proceedings in Current Issues in Statistical Shape Analysis* (ed. by K. V. Mardia and C. A. Gill), pp. 139–153. Leeds University Press, Leeds.

Bookstein F.L. and Green W.D.K. (1993a) A feature space for edgels in images with landmarks, *J. Math. Imaging and Vision*, **3**, 231–261.

Bookstein, F.L. and Green W.D.K. (1993b) A feature space for derivatives of deformations. In: *Information Processing in Medical Imaging: IPMI 93. Lecture Notes in Computer Science*, (ed. by H. Barrett and A. Gmitro), vol. 687, pp. 1–16. Springer-Verlag, Berlin.

Bookstein F.L. and Green W.D.K. (1994a) Edgewarp: A flexible program package for biometric image warping in two dimensions. In: *Visualization in Biomedical Computing 1994. S.P.I.E. Proceedings* (ed. by R. Robb), v. 2359, pp. 135–147.

Bookstein F.L. and Green W.D.K. (1994b) *Edgewarp: A program for biometric warping of medical images.* Videotape, 26 min.

Cutting C.B., Bookstein F., Haddad B., Dean D. and Kim D. (1993) A spline-based approach for averaging three-dimensional curves and surfaces. In: *Mathematical Methods in Medical Imaging* II (ed. by J.N. Wilson and D. C. Wilson), *SPIE Proc.*, **2035**, 29–44..

Dean D. and Marcus L. (1995) Chi-square test of biological space curve affinities. In *Advances in Morphometrics: Proc. 1993 NATO ASI on Morphometrics* (ed. by L. Marcus *et al.*). Plenum, in press.

Galton Sir Francis (1987) Classification of portraits, *Nature*, **76**, 617–618.

Goodall C.R. (1991) Procrustes methods in the statistical analysis of shape, *J. R. Stat. Soc.*, **B53**, 285–339.

Goodall C.R. and Mardia K. (1993) Multivariate aspects of shape theory, *Annls. Stat.*, **21**, 848–866.

Grenander U., Chow Y. and Keenan, D. (1991) *Hands: A Pattern Theoretic Study of Biological Shapes.* Springer, Berlin.

Grenander U. and Miller M. (1994) Representations of knowledge in complex systems, *J. R. Stat. Soc., Ser. B*, **56**, 549–603.

Kendall D.G. (1984) Shape-manifolds, procrustean metrics, and complex projective spaces, *Bull. London Math. Soc.*, **16**, 81–121.

Kent J.T. (1994) The complex Bingham distribution and shape analysis, *J. R. Stat. Soc.*, **B56**, 285–299.

Kent J.T. (1995) Current issues for statistical inference in shape analysis. In: *Proc. Curr. Issues Stat. Shape Analysis* (ed. by K.V. Mardia and C.A. Gill), pp. 167–173. Leeds University Press, Leeds.

Kent J.T. and Mardia K.V. (1995) Consistency of Procrustes estimators. Completed manuscript.

Lohmann G.P. (1983) Eigenshape analysis of microfossils: a general morphometric procedure for describing changes in shape, *Math. Geol.*, **15**, 659–672.

Lohmann G.P. and Schweitzer P. (1990) On eigenshape analysis. In: *Proceedings of the Michigan Morphometrics Workshop* (ed. by F.J. Rohlf and F. Bookstein), pp. 147–166. University of Michigan Museums, Ann Arbor.

Marcus L.F. Bello E. and García-Valdecasas A. (eds) (1993) *Contributions to Morphometrics.* Monografias, Museo Nacional de Ciencias Naturales, Consejo Superior de Investigaciones Cientificas, Madrid,

Marcus L.F., Corti M., Loy A., Naylor G. and Slice D. (eds) (1995) *Advances in Morphometrics: Proc. 1993 NATO ASI on Morphometrics.* Plenum, to appear.

Mardia K.V. (1995) Shape advances and future perspectives. In: *Proc. Curr. Issues in Statistical Shape Analysis* (ed. by K.V. Mardia and C.A. Gill), pp. 57–75. Leeds University Press, Leeds.

Reyment R., Blackith, R. and Campbell, N. (1984) *Multivariate Morphometrics*, 2nd edn. Academic Press, New York.

Reyment, R. and Jöreskog, K. (1993) *Applied Factor Analysis in the Natural Sciences.* Cambridge University Press, Cambridge.

Rohlf F.J. (1990) Fitting curves to outlines. In *Proc. Michigan Morphometrics Workshop* (ed. by Rohlf F.J. and Bookstein F.) University of Michigan Museums, Ann Arbor.

Rohlf F.J. (1993) Relative warp analysis and an example of its application to mosquito wings. In: *Contributions to Morphometrics* (ed. by L. Marcus *et al.*). Monografias, pp. 131–159. Museo Nacional de Ciencias Naturales, Consejo Superior de Investigaciones Cientificas, Madrid.

Rohlf F.J. and Bookstein F. L. (1990) *Proceedings of the Michigan Morphometrics Workshop.* University of Michigan Museums, Ann Arbor.

Rohlf F.J. and Slice D. (1990) Extensions of the Procrustes method for the optimal superposition of landmarks, *Syst. Zool.*, **39**, 40–59.

Sampson P.D., Bookstein, F.L., Sheehan F. and Bolson E. (1995) Eigenshape analysis of left ventricular function from contrast ventriculograms. In: *Advances in Morphometrics: Proc. 1993 NATO ASI on Morphometrics* (ed. by L. Marcus *et al.*). Plenum, New York.

Thompson D'A.W. (1917) *On Growth and Form.* Macmillan, London.

Manuscript received 17 February 1995; revision accepted 16 March 1995